World Journal of Gastroenterology

Submit a Manuscript: http://www.wjgnet.com/esps/
Help Desk: http://www.wjgnet.com/esps/helpdesk.aspx
DOI: 10.3748/wjg.v22.i1.205

World J Gastroenterol 2016 January 7; 22(1): 205-220
ISSN 1007-9327 (print) ISSN 2219-2840 (online)

TOPIC HIGHLIGHT

2016 Hepatocellular Carcinoma: Global view

Advances in computed tomography and magnetic resonance imaging of hepatocellular carcinoma

Tiffany Hennedige, Sudhakar K Venkatesh

Tiffany Hennedige, Department of Oncologic Imaging, National Cancer Centre, Singapore 169610, Singapore

Sudhakar K Venkatesh, Department of Radiology, Mayo Clinic, MN 55905, United States

Author contributions: Hennedige T and Venkatesh SK analyzed the literature and wrote the manuscript.

Conflict-of-interest statement: The authors have no conflict of interest to report.

Correspondence to: Sudhakar K Venkatesh, MD, FRCR, Department of Radiology, Mayo Clinic, 200, First Street SW, Rochester, MN 55905,
United States. venkatesh.sudhakar@mayo.edu
Telephone: +1-507-2841728
Fax: +1-507-2842405

Received: May 29, 2015
Peer-review started: June 1, 2015
First decision: July 14, 2015
Revised: August 4, 2015
Accepted: December 1, 2015
Article in press: December 1, 2015
Published online: January 7, 2016

Abstract

Hepatocellular carcinoma (HCC) is the most common primary liver cancer. Imaging is important for establishing a diagnosis of HCC and early diagnosis is imperative as several potentially curative treatments are available when HCC is small. Hepatocarcinogenesis occurs in a stepwise manner on a background of chronic liver disease or cirrhosis wherein multiple genes are altered resulting in a range of cirrhosis-associated nodules. This progression is related to increased cellularity, neovascularity and size of the nodule. An understanding of the stepwise progression may aid in early diagnosis. Dynamic and multiphase contrast-enhanced computed tomography and magnetic resonance imaging still form the cornerstone in the diagnosis of HCC. An overview of the current diagnostic standards of HCC in accordance to the more common practicing guidelines and their differences will be reviewed. Ancillary features contribute to diagnostic confidence and has been incorporated into the more recent Liver Imaging Reporting and Data System. The use of hepatocyte-specific contrast agents is increasing and gradually changing the standard of diagnosis of HCC; the most significant benefit being the lack of uptake in the hepatocyte phase in the earlier stages of HCC progression. An outline of supplementary techniques in the imaging of HCC will also be reviewed.

Key words: Hepatocellular carcinoma; Computed tomography; Magnetic resonance imaging; Contrast agent; Cirrhosis; Ancillary features

Core tip: Imaging is important for establishing a diagnosis of hepatocellular carcinoma (HCC) and an understanding of the stepwise progression of hepatocarcinogenesis may aid in early diagnosis. Dynamic and multiphase contrast-enhanced computed tomography and magnetic resonance imaging still form the cornerstone in the diagnosis of HCC. An overview of the current diagnostic standards of HCC in accordance to the more common practicing guidelines and their differences will be reviewed. Various ancillary

features, use of hepatocyte-specific contrast agents and supplementary imaging techniques also help to increase diagnostic confidence and will be reviewed.

Hennedige T, Venkatesh SK. Advances in computed tomography and magnetic resonance imaging of hepatocellular carcinoma. *World J Gastroenterol* 2016; 22(1): 205-220 Available from: URL: http://www.wjgnet.com/1007-9327/full/v22/i1/205.htm DOI: http://dx.doi.org/10.3748/wjg.v22.i1.205

INTRODUCTION

Hepatocellular carcinoma (HCC) is the most common primary liver cancer. It ranks sixth in cancer incidence and third in cancer mortality worldwide[1]. It is the most prevalent liver cancer with up to three-quarter of cases in the world occurring in Asia due to the high prevalence of chronic viral hepatitis B[2]. Patients diagnosed with HCC generally have a poor prognosis due to the aggressive nature of the disease[3]. Early diagnosis of HCC is imperative as several potentially curative treatments are available, especially when the lesion is small.

Regular surveillance of patients is instituted for early detection of HCC in patients with chronic liver disease and particularly in those with advanced liver fibrosis. Screening involves clinical examination, serum analysis of liver function and tumour antigens such as alpha-fetoprotein (AFP) and imaging. Although AFP is not specific for HCC and may give false positive results in the setting of hepatitis and fibrosis, it is still useful in monitoring of the disease process in combination with imaging[4]. Non-invasive diagnosis with imaging is currently the preferred method and several guidelines are available to aid in diagnosis and they all endorse arterial enhancement followed by washout in the diagnosis of HCC (Figure 1). Dynamic and multiphase contrast-enhanced computed tomography (CT) and magnetic resonance imaging (MRI) form the cornerstone of diagnosis in HCC. This review presents an overview of the current diagnostic standards of HCC in accordance to the more common practicing guidelines as well as the use of ancillary features and hepatocyte-specific contrast agents in the diagnosis of HCC. An outline of supplementary techniques in the imaging of HCC will also be reviewed.

EPIDEMIOLOGY

HCC is associated with chronic liver disease and cirrhosis irrespective of its etiology. It has been shown that only about 10% of HCCs develop in non-cirrhotic livers[5]. The incidence of HCC has been increasing, with chronic hepatitis B and C infections being major contributory factors worldwide[6]. Apart from chronic viral infection, several lifestyle factors contribute to the development of HCC. These include excessive alcohol consumption, obesity, diabetes and intake of aflatoxin-contaminated foods[7]. Greater than 90% of HCC cases develop in chronically inflamed liver as a result of viral hepatitis and alcohol abuse[8]. Obesity and diabetes are associated with development of non-alcoholic fatty liver disease (NAFLD)[9]. Insulin resistance and the resulting inflammatory cascade together with the development of non-alcoholic steatohepatitis (NASH) appear to encourage hepatocarcinogenesis[10]. Cigarette smoking is regarded as a co-factor in the development of HCC[11]. Hepatocarcinogenesis also increases in the setting of HIV infection[12]. Lastly, genetic conditions such as haemochromatosis, glycogen storage disease type 1, alpha 1-antitrypsin deficiency are all associated with increased risk of HCC, most frequently on a background of cirrhosis[13].

PATHOGENESIS

In patients with chronic liver disease, HCC typically develops in a stepwise manner wherein multiple genes are altered. Chronic inflammation and regeneration of hepatocytes are underlying causes; it results in damage to the DNA of regenerating hepatocytes hence increasing the chance of gene alterations associated with carcinogenesis[14]. The currently accepted nomenclature for stepwise carcinogenesis of HCC is: regenerative nodule (RN); low-grade dysplastic nodule (DNI); high-grade dysplastic nodule (DNII); early and progressed HCC[15-17].

Regenerative nodules

These are typically well-defined rounded regions of the cirrhotic parenchyma surrounded by scar tissue[18]. RNs are essentially phenotypically normal and are usually considered benign lesions[19]. Relative to background parenchyma, they are typically isoattenuating on unenhanced CT, T1, T2 and diffusion weighted (DWI) MR imaging[20,21] (Figure 2). On occasion, they may be T1 hyperintense and T2 hypointense, similar to dysplastic nodules[22]. With intravenous extracellular contrast injection, most RN enhance to the same degree as adjacent liver parenchyma or show slightly less enhancement, hence, they may appear as mildly hypoattenuating nodules relative to enhancing fibrosis in the portal venous phase[23] (Figure 3).

Dysplastic nodules

These are nodular lesions that differ macroscopically and microscopically from background parenchyma[24]. They are classified as low or high grade depending on the presence of cytologic and architectural aberrations[25]. DNI resemble RN histologically except that they contain unpaired arteries and clone-like populations[24,25]. On the other hand, DNII show features similar to that of a well-differentiated HCC. They demonstrate cellular atypia with clone-like features, expansile subnodules and

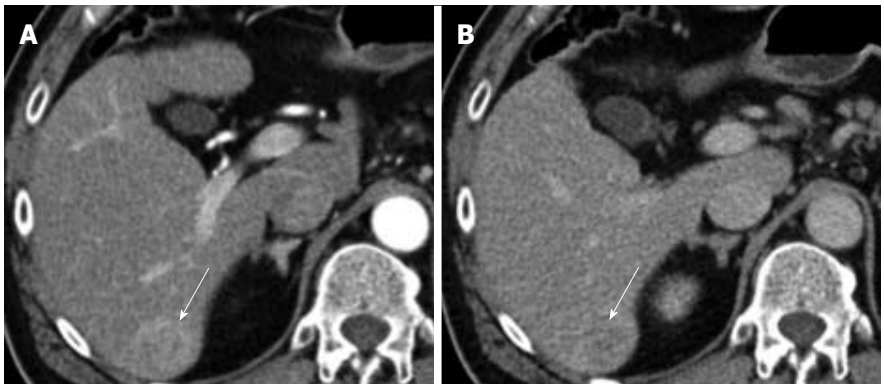

Figure 1 Typical features of arterial enhancement (A) with washout in the portal venous phase (B) is noted in segment 6 in keeping with histological-proven hepatocellular carcinoma.

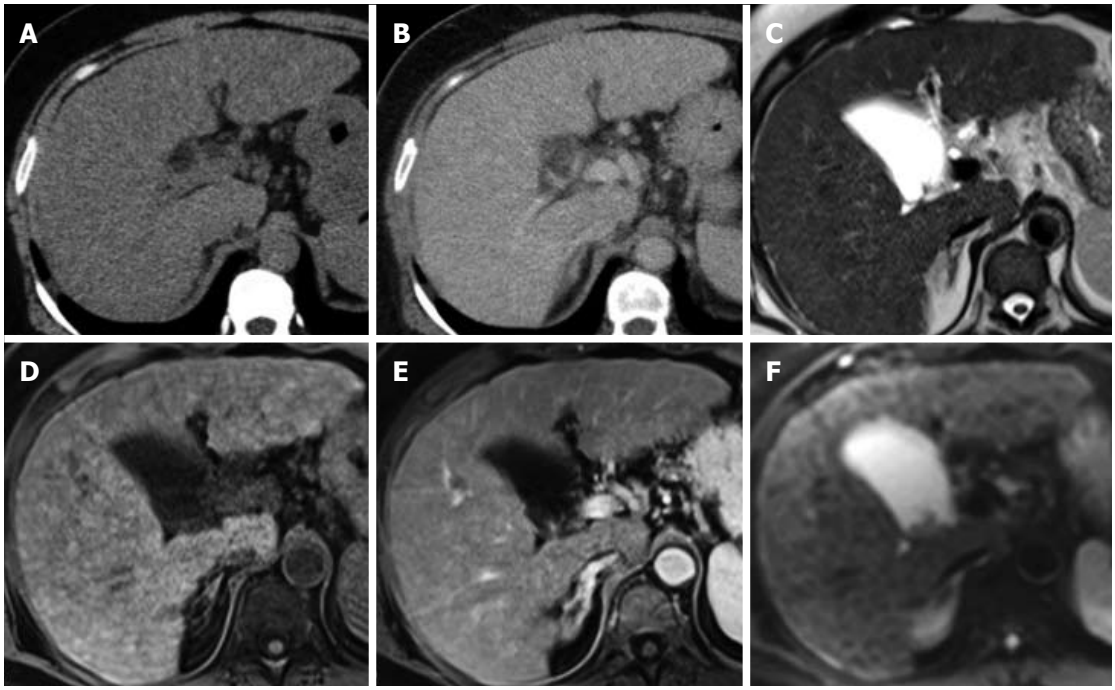

Figure 2 The liver demonstrates a nodular outline consistent with cirrhosis and multiple small regenerative nodules that are isodense on unenhanced (A) and portal venous phase (B) on computed tomography, predominantly isointense on T2W (C) and T1W (D) sequences with no evidence of arterial enhancement (E) or restricted diffusion (F).

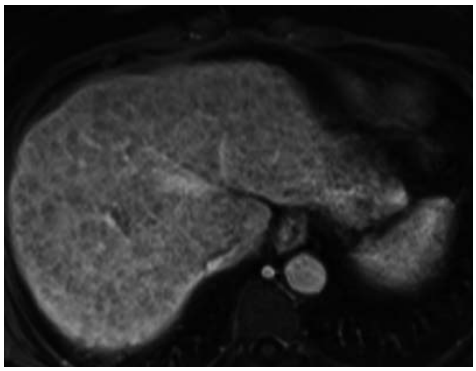

Figure 3 Multiple regenerative nodules in the portal venous phase may appear mildly hypoattenuating relative to enhancing fibrosis.

architectural alterations[25,26]. Some DNII may contain subnodules of HCC resulting in the nodule-in-nodule appearance[27]. On CT, most DN are hypo- or isodense in the arterial, portal venous and delayed phases[28]. They are typically T1 hyperintense and iso- to hypointense on T2 imaging[23] (Figure 4). Some, especially DNII may contain intracellular fat resulting in signal loss on out-of-phase images[29]. Unlike HCC, DN are almost never T2 hyperintense or show restricted diffusion[30,31] (Figure 4).

Early HCC

Early HCC is likened to carcinoma-*in-situ* of other organs[32]. They rarely exceed 2 cm and unlike progressed HCC which displaces and destroys sur-

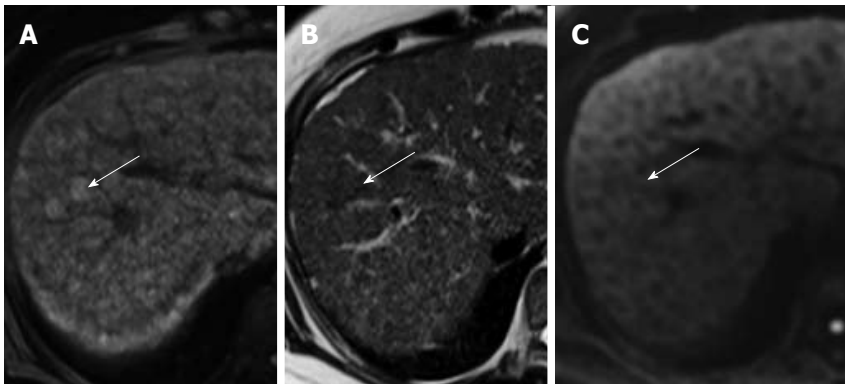

Figure 4 Dysplastic nodules may appears hyperintense on T1W (A), iso-hypointense on T2W (B) but do not show restricted diffusion (C).

rounding liver parenchyma, early HCCs expand by gradually replacing the parenchyma[17]. The main distinguishing characteristic between a DNII and early HCC is the presence of stromal invasion in the latter which is defined as infiltration of tumour cells into fibrous tissue surrounding portal tracts[25].

Progressed HCC

Theses nodules are overtly malignant with propensity to invade vessels and metastasize. Lesions smaller than 2 cm are typically distinctly nodular with well-defined margins; they grow by expanding into and compressing surrounding parenchyma resulting in formation of a pseudocapsule[17]. Lesions larger than 2 cm demonstrate a more aggressive behaviour. A mosaic pattern is characteristic which is defined by the presence of several internal subnodules separated by fibrous septa as well as areas of necrosis, haemorrhage and occasionally fatty metamorphosis[33].

CURRENT DIAGNOSTIC STANDARDS OF HCC ACCORDING TO EXISTING GUIDELINES

In oncology, the diagnosis of malignancy usually necessitates tissue sampling prior to determination of treatment approach. Characterisation of HCC however, is an exception as a non-invasive diagnosis can be attained with imaging in high-risk patient populations[2,34,35]. The more widely used guidelines are the European Association for the Study of the Liver (EASL)[34], American Association for the Study of Liver Disease (AASLD)[35] and the Asian Pacific Society for the Study of the Liver (APASL)[2]. The hallmark diagnostic characteristics of HCC are arterial enhancement followed by portal venous and/or delayed phase washout[36-38] (Figures 1 and 5), this is common to all three guidelines. Comparative studies for CT and MR imaging using extracellular contrast agents found higher sensitivities with MR imaging[39,40]. The sensitivity of MRI for nodular HCC of all sizes is 77%-100% while that of CT is 68%-91%[34,35,41,42]. The size of the lesion is an important determinant in diagnosis; for lesions larger than 2 cm, the sensitivity is close to 100% for both modalities but drops to 45%-80% with MRI and 40%-75% with CT for lesions measuring 1-2 cm[40,43].

Both EASL and AASLD stratify lesions according to size; < 1 cm, 1-2 cm and > 2 cm for EASL and < 1 cm and > 1 cm for AASLD. Both guidelines deem less than 1 cm lesions as too small for characterisation and recommend follow-up. The diagnosis of HCC in lesions larger than 2 cm requires only a single imaging modality when the hallmark enhancement characteristics are present. Another imaging technique should be performed when enhancement characteristics are atypical. These guidelines differ with respect to lesions between 1-2 cm; the AASLD recommends the same approaches as for lesions larger than 2cm whereas EASL recommends the presence of typical enhancement characteristics on two imaging modalities. Both EASL and AASLD recommend biopsy in patients with lesions that do not fit in the above imaging criteria. Unlike EASL and AASLD, APASL does not stratify lesions according to size. Also, the APASL acknowledges the use of contrast-enhanced ultrasound (CEUS) to depict hypervascularity in lesions hypovascular on CT or MRI. When a defect is observed in the Kupffer phase on CEUS, it is diagnosed as HCC. The Kupffer phase also known as the post-vascular phase which occurs 20 min after injection and implies the presence of Kupffer cells which are present in non-neoplastic liver parenchyma and reduced in HCC[44]. If this defect is not observed, close follow-up is recommended.

The Liver Imaging Reporting and Data System (Li-RADS)[45] was introduced relatively recently by the American College of Radiology. The aim of this system was to standardize terminology and criteria in reporting of liver lesions in chronic liver disease. Each lesion is assigned a category ranging from L1 to L5, with each category denoting a higher probability of HCC. Unlike the above mentioned guidelines, Li-

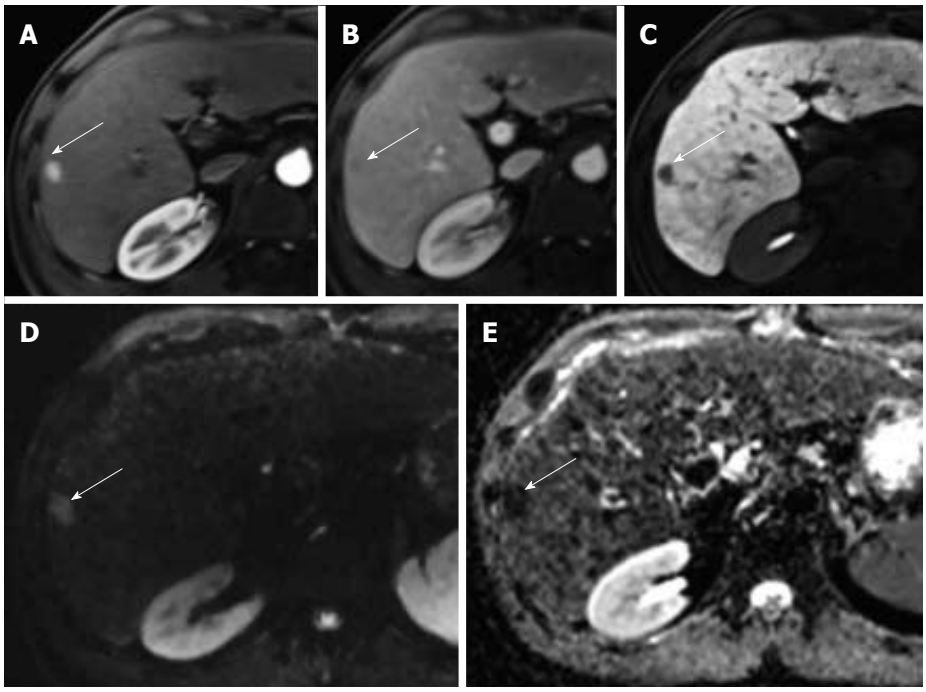

Figure 5 Typical characteristics of a hepatocellular carcinoma. A small lesion in segment 6 demonstrates arterial enhancement (A), washout in the portal venous phase (B), hypointensity in the hepatobiliary phase (C) and restricted diffusion [hyperintense on DWI (D) and hypointense on ADC (E)].

Table 1 The Liver Imaging Reporting and Data System

		Arterial phase hypo- or iso-enhancement		Arterial phase hyper-enhancement		
Diameter (mm)		< 20	⩾ 20	< 10	10-19	⩾ 20
Washout	None	L3	L3	L3	L3	L4
Capsule formation	One	L3	L4	L4	L4/L5	L5
Threshold growth	⩾ Two	L4	L4	L4	L5	L5

Modified from URL: http://www.acr.org/Quality-Safety/Resources/LIRADS/.

RADS takes into account ancillary features. The diagnosis of HCC is established by a combination of major signs including: arterial phase enhancement, lesion size, washout, capsule formation and threshold growth (Table 1). Ancillary features are then applied to upgrade or downgrade the initial classification.

ANCILLARY FEATURES

A substantial proportion of HCCs do not demonstrate the typical arterial enhancement with subsequent washout pattern. It has been shown that up to 40% of HCC lack arterial phase enhancement[34], these are largely early or poorly-differentiated infiltrative HCCs[46,47]. Also, 40%-60% of small HCCs do not demonstrate subsequent washout[48,49]. Hence, several ancillary signs have been described, most of which are better depicted with MRI. It is important to emphasise that these features individually are not specific for HCC, but their presence increases diagnostic probability.

Restricted diffusion

DWI assesses molecular water motion within tissues and this information is acquired by applying balanced gradients to T2-weighted sequences. The degree of diffusion weighting can be altered by changing the *b* value, an acquisition parameter. With DWI, signal intensity from stationary water molecules is preserved whilst those that are in motion lose signal intensity depending on the degree of motion from their original position at the time of signal acquisition. Diffusion restriction is more prominent in malignant than in benign tumours[50]; the combination of high cellularity and intact cell membranes restrict the motion of water molecules resulting in hyperintensity on diffusion weighted imaging (DWI) and reduction in apparent diffusion coefficient (ADC) maps. DWI is particularly useful in the initial screening of the liver as nearly 70%-95% of HCCs can appear hyperintense[51-53], particularly using low *b* values[54]. The presence of restricted diffusion is found to be especially useful in the characterisation of small lesions[55,56] (Figure 5). Intermediate or poorly-differentiated HCCs are more often hyperintense on DWI than well-differentiated HCC[16]. In addition, restricted diffusion may be useful in the diagnosis of bland versus tumour thrombus[16].

Intralesional fat

The presence of fat in a focal liver lesion is better appreciated on MRI than on CT. The presence of fat is depicted as signal drop-out in the opposed-phase images (Figure 6). In chronic liver disease, a fat-contained tumour is highly suggestive of HCC[42],

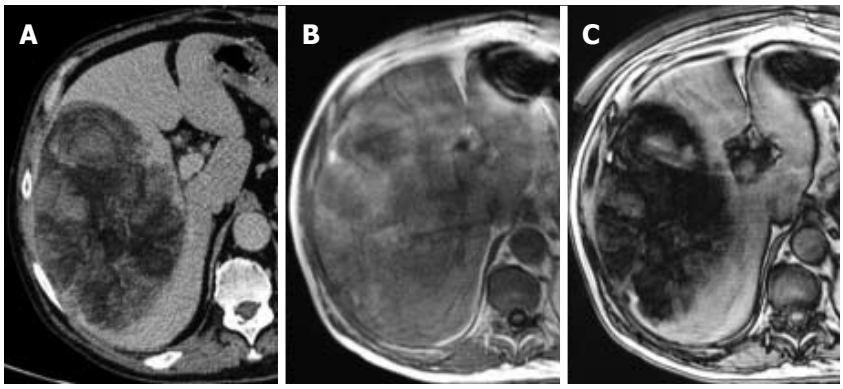

Figure 6 A large hepatocellular carcinoma in the right lobe of the liver demonstrates fat attenuation on non-contrast enhanced computed tomography (A), and loss of signal in the in- (B) and opposed-phase (C) images indicative of fat.

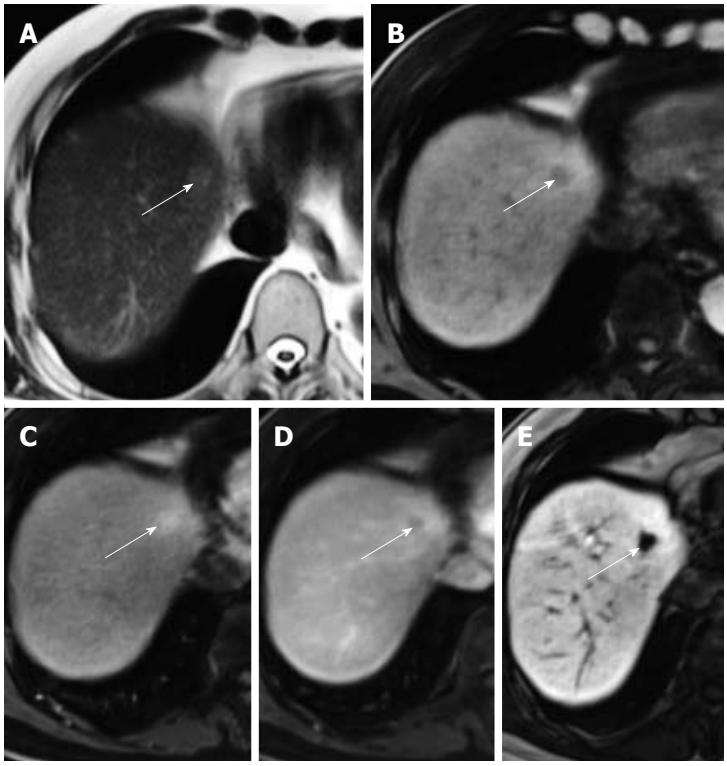

Figure 7 A small hepatocellular carcinoma demonstrates mild T2W hyperintensity (A), T1W hypointensity (B), arterial enhancement (C), portal venous phase washout (D) and hypointensity on the 20 min hepatobiliary phase (E) after injection with Gd-EOB-DTPA.

however, benign fat-containing regenerative nodules may also be seen[16]. Intralesional fat is more commonly seen in early as opposed to progressed HCC, with better prognosis associated with fat-contained HCC[55].

Mild to moderate T2 signal intensity

On MRI, the presence of mild to moderate T2 signal intensity is more often seen in HCCs (Figure 7). Markedly T2 hyperintense lesions are more likely to represent benign lesions such as cysts and haemangiomas, whereas T2 hypointense lesions may represent iron deposition in the nodules. Like the presence of intralesional fat, the degree of T2 signal intensity may have prognostic implications; many well-differentiated HCCs are found to be hypo- or isointense[56].

Mosaic pattern

The variable tissue components of HCC account for this mosaic pattern; enhancing areas indicate viable tumour cells and low attenuation foci represent necrosis, fibrosis or hemorrhage[33]. Most large HCCs present with this pattern and it is regarded as fairly specific (Figure 8). Since it is found primarily in large lesions, the utility of this ancillary sign is probably of less utility in the characterisation of small HCCs.

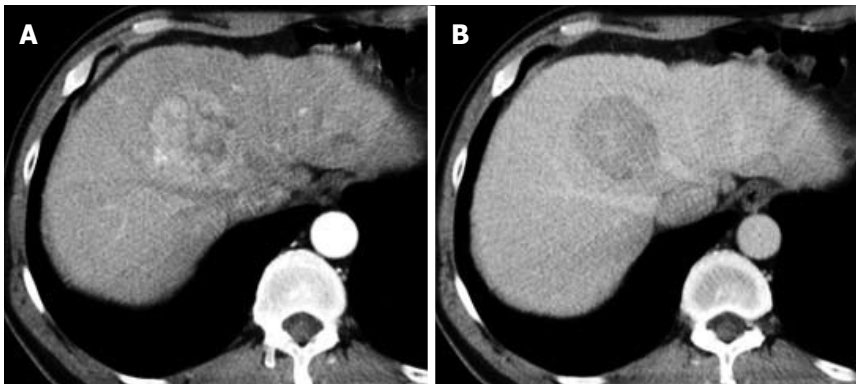

Figure 8 Mosaic attenuation is demonstrated on the arterial phase sequence (A) in this relatively large hepatocellular carcinoma followed by washout (B).

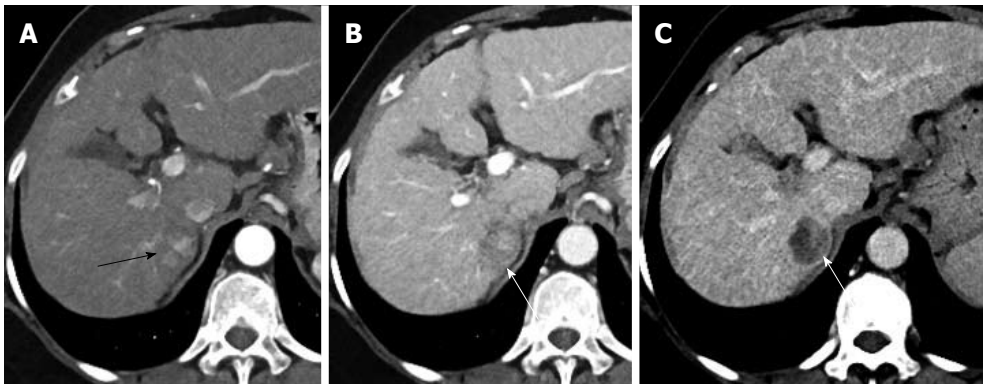

Figure 9 Cirrhotic liver with an arterially-enhancing lesion (black arrow) in segment 6 (A), which demonstrates a thin pseudocapsule (white arrow) in the portal venous (B) and delayed phases (C), better appreciated in the latter.

Pseudocapsule

This refers to a rim of peripheral enhancement in the portal venous or delayed phases (Figure 9). This sign may be well depicted in both CT and MRI and has been shown to be a significant predictor in the diagnosis of HCC[42,49]. A pseudocapsule has been found in 10%-47% of cases depending on the series studied[57-59].

Vascular invasion

Portal vein tumour thrombus (PVTT) is a well-known complication of HCCs; such invasion helps distinguish HCC from secondary hepatic cancers which rarely invade intrahepatic vessels[60]. It is important to note that the presence of a tumour thrombus can modify typical imaging features of HCC. When HCC infiltrates a portal vein, it continues to receive arterial blood supply and the tumor may drain directly into the portal vein. This direct draining results in arterioportal shunting and changes in portal vein haemodynamics[61]. Large HCCs complicated by PVTT less often demonstrate typical arterial enhancement with subsequent washout. Instead, the PVTT itself can show arterial phase enhancement with subsequent washout with distension of the vein (Figure 10)[61]. This arterioportal shunting may also result in poor enhancement of the surrounding liver parenchyma.

Lack of iron content

Presence of iron is better appreciated on MRI as opposed to CT and is shown as marked hypointensity on T2W sequences. Iron is normally present in the Kupffer cells that reside in sinusoids and are abundant in normal liver parenchyma. The presence of iron is highly suggestive of a non-malignant lesion in a cirrhotic liver[48]. On the contrary, the presence of an iron-free lesion in an otherwise iron-laden liver may suggest HCC (Figure 11).

Nodule-in-nodule appearance

This refers to the presence of a nodule within a larger nodule and is usually the result of the development of HCC within a pre-existing cirrhosis-related nodule. The nodule within the larger lesion may demonstrate increased arterial enhancement or T2 signal intensity relative to the surrounding larger nodule (Figure 12).

USE OF HEPATOBILIARY CONTRAST AGENTS

Hepatobiliary MRI contrast agents are increasingly being used and gradually changing the standard of diagnosis of HCC. These agents are gadolinium chelate-based with an initial vascular phase that is

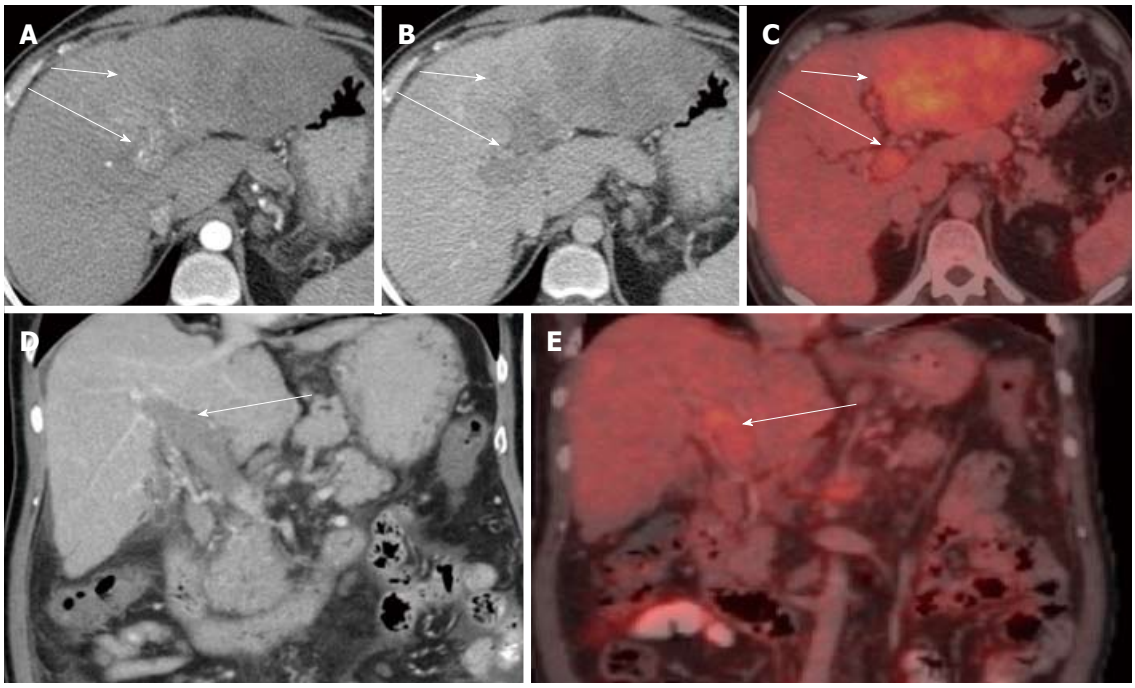

Figure 10 Vascular invasion. A large ill-defined left lobe mass with no significant arterial enhancement (A) and washout in the portal venous phase (B). An FDG-PET CT was done which revealed uptake in the left lobe mass (C) consistent with a hypermetabolic tumour. Arterial enhancement is noted within the distended thrombus filled portal veins in (A) with subsequent washout (B) suggestive of tumour thrombus. The tumour thrombus also demonstrates increased uptake on FDG-PET (C). Coronal images better depict the distended thrombus filled portal vein (D) with increased uptake on PET/CT (E) (short arrow: tumour; long arrow: tumour thrombus). PET: Positron emission tomography; CT: Computed tomography; FDG: Fluoro-2-deoxy-D-glucose.

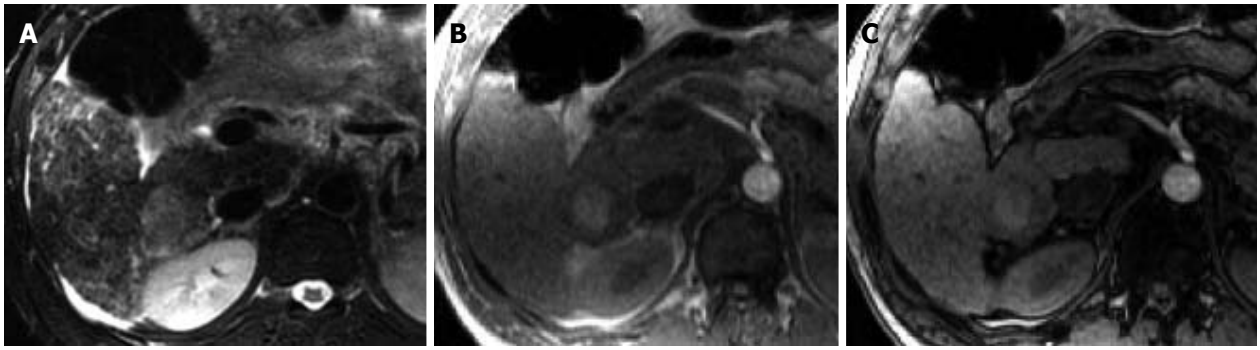

Figure 11 An iron-laden liver in a patient with hemochromatosis demonstrates a T2W hyperintense lesion (A) which is iron-free in the in- (B) and opposed (C) phases suggestive of hepatocellular carcinoma.

similar to the extracellular agents. However, they are actively taken up by hepatocytes *via* a group of proteins expressed in hepatocytes along the sinusoidal membrane known as organic anionic transporting polypeptides (OATP)[16]. In humans, OATP 8 appears to be responsible for cellular uptake[62]. The contrast agents are then partially excreted into the biliary system. Two hepatobiliary MRI contrast agents are currently in use: gadobenate dimeglumine (Gd-BOPTA, Multihance, Bracco, Milan, Italy) and gadoxetate dimeglumine (Gd-EOB-DTPA, Primovist in Europe and Eovist in the United States, Bayer Healthcare). Both contrast agents can be injected as an intravenous bolus dose. The hepatobiliary phase is attained 1-3 h after injection of Gd-BOPTA and about 20 min after injection of Gd-EOB-DTPA. With Gd-BOPTA, only 5% of the drug is transported through hepatocytes and excreted into bile whereas with Gd-EOB-DTPA, approximately 50% of the drug undergoes biliary excretion.

A small dose of Gd-EOB-DTPA (0.025 mmol/kg) is required compared to 0.1 mmol/kg for Gd-BOPTA. The former therefore has significant advantages in terms of safety, timing of examination and potentially better contrast. However, due to the low volume injected with Gd-EOB-DTPA compared to Gd-BOPTA, the vascular phase images are less ideal with a narrower imaging window for late hepatic arterial phase acquisition[63] which is when peak arterial enhancement of a nodule typically occurs. This can be overcome by performing multiple acquisitions during the arterial phase. Gd-EOB-DTPA does not provide a conventional delayed phase

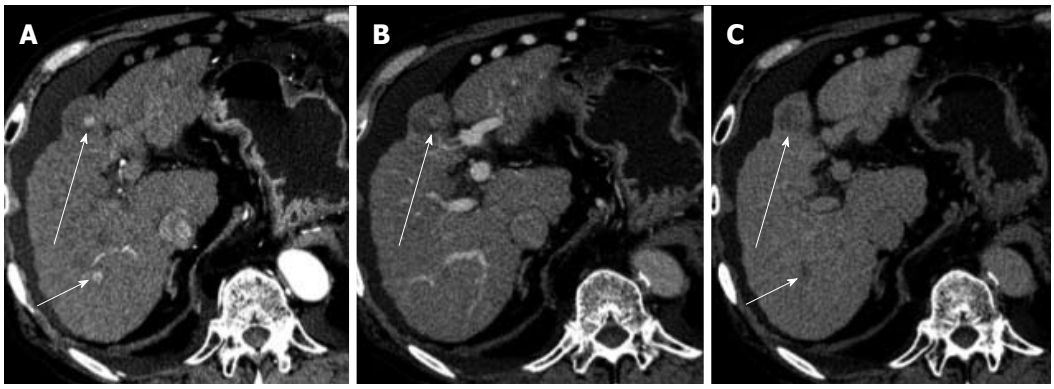

Figure 12 A focus of arterial enhancement is noted within a larger hypodense nodule (A) which demonstrates washout in the portal venous (B) and delayed (C) phases suggestive of development of hepatocellular carcinoma within a pre-existing cirrhosis-related nodule (long arrow). Another focus of hepatocellular carcinoma (short arrow) is noted more posteriorly demonstrating arterial enhancement (A) and delayed phase wash-out (C).

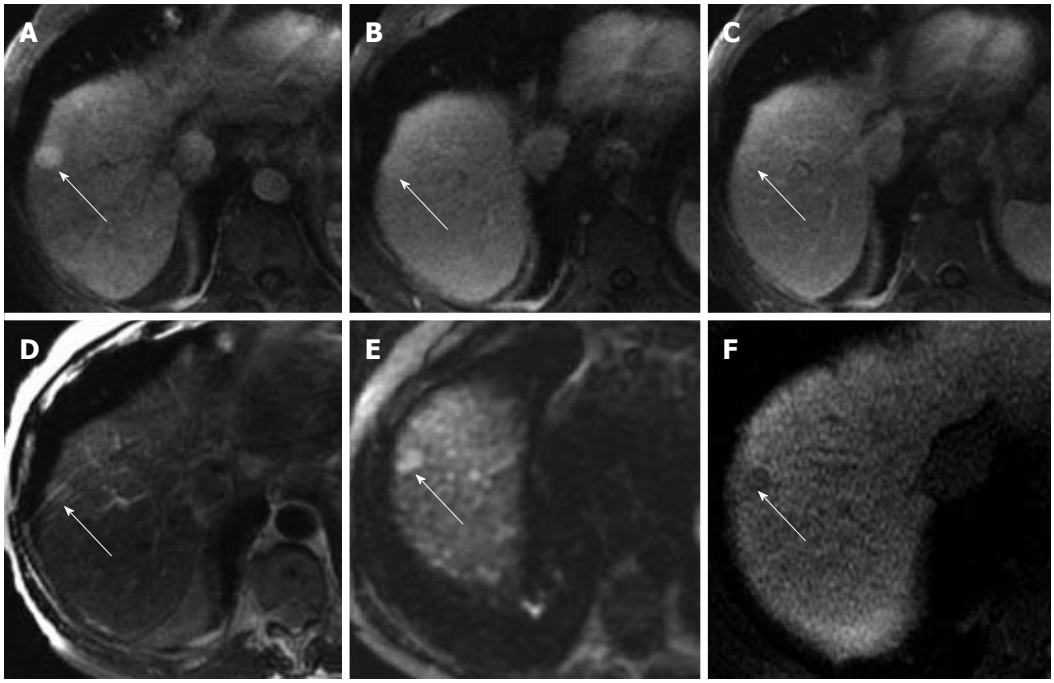

Figure 13 An initial study was performed using Gd-DTPA. This showed an arterially-enhancing lesion (A) with no evidence of wash-out or pseudocapsule on the portal venous (B) or delayed (C) phases with hyperintensity on T2W (D) and DWI (E) sequences. A follow-up study acquired two months later with Gd-EOB-DTPA demonstrated a hypointense lesion on the hepatobiliary phase (F), increasing diagnostic confidence of hepatocellular carcinoma.

as hepatocellular uptake occurs during its first pass through the hepatic sinusoids[64]. Hence, by the end of the portal venous phase, considerable hepatocellular uptake has occurred with both intracellular and extracellular pools of Gd-EOB-DTPA contributing substantially to parenchymal enhancement[64]. As this phase represents a transition from extracellular-dominant to intracellular-dominant enhancement, it may be termed the transitional phase[65].

In addition to increased cellularity and neovascularity in the multistep carcinogenesis of HCC, OATP expression gradually decreases in the development of HCC. This results in a lack of uptake in the hepatobiliary phase; most HCCs are hypointense in the hepatobiliary phase (Figure 7) whereas most non-HCC cirrhosis-associated nodules are iso- or hyperintense secondary to preservation of OATP 8 expression[66]. It is however important to note that 5%-10% of HCCs are iso- or hyperintense to liver in the hepatobiliary phase[67,68]. The addition of hepatobiliary phase sequences improves sensitivity of diagnosis of HCC by 5%-15% with Gd-EOB-DTPA (Figure 13)[69,70] and around 10% with Gd-BOPTA[71]. Interestingly, a study showed that 96% of HCC lacking arterial enhancement with subsequent washout (seen primarily in early HCCs) were hypointense during the hepatobiliary phase[72]. This is likely the most significant benefit of the use of hepatobiliary contrast agents in determination of HCC. It is important to note however that all non-hepatocellular lesions appear hypointense

on the hepatobiliary phase. Hence, it is imperative to interpret this phase in conjunction with that of the other sequences.

SUPPLEMENTARY IMAGING TECHNIQUES

Utility of non-contrast enhanced phase

Addition of a non-contrast enhanced phase (NC-CT) to a multi-phase CT study has been found to useful in providing a baseline for assessment of arterial phase enhancement and improving diagnosis of HCC[73]. The current practice of characterizing enhancement and washout with dynamic CT is performed qualitatively by visual assessment of the lesion relative to the surrounding liver parenchyma. This assessment is thus dependent upon variables that can influence liver attenuation such as steatosis and iron deposition. With the addition of NC-CT, even if a lesion was found to be isodense on the arterial phase, the observation of hypodensity on NC-CT would imply hypervascularity of the lesion.

Perfusion imaging

The improved temporal resolution of newer and faster multidetector CT systems allows perfusion studies of the liver[74]. CT perfusion is a method to analyze hemodynamic changes in tissue; it allows for quantitative assessment of various parameters such as tumour blood flow, blood volume, mean transit time and permeability-surface area product[75]. The liver has dual blood supply and neoarterialization occurs with the development of HCC resulting in alteration of perfusion parameters. Blood flow, blood volume, arterial perfusion and hepatic perfusion index were found to be significantly higher in HCC relative to hepatic parenchyma[76,77]. Sahani *et al*[75] also found that mean blood flow, blood volume and permeability-surface area product were higher in well-differentiated HCC than in moderately or poorly differentiated tumours. Additionally, it has been suggested that perfusion parameters can be utilized as biomakers to monitor treatment response in tumours[78].

Dual-energy CT

Conventional MDCT uses a polychromatic X-ray spectrum provided by a single X-ray tube whereas dual-energy CT (DECT) uses two different energy spectra produced by two different kVp settings. This is achieved by using two X-ray tubes at different tube currents with two corresponding detectors or with a single source X-ray tube with fast peak kVp switching. It is based on the premise that tissues demonstrate different attenuation at different energy levels. This allows for enhanced tissue differentiation and characterization, reduction of artifacts, iodine conspicuity and improvement of contrast-to-noise ratio (CNR) and signal-to-noise ratio (SNR)[79]. The attenuation of a material increases as its photon energy decreases. Materials with higher atomic numbers, such as iodine, portray a much greater attenuation increase as the photon energy decreases. This provides the basis for greater attenuation separation between tumour and liver parenchyma[80]. Gao *et al*[81] found that monochromatic images obtained using single source DECT can enhance the CT attenuation of iodine contrast media at lower energy levels in the enhanced arterial phase which aids in the identification of more and smaller HCC lesions (Figure 14). DECT may also improve detection of fat within hepatic lesions which may be indicative of HCC[82].

MR elastography

MR elastography (MRE) is a technique which is used for quantitative assessment of tissue stiffness and its most common clinical application is for evaluation of liver stiffness in the diagnosis of hepatic fibrosis[83]. In this technique, hepatic stiffness is measured using low-frequency mechanical shear waves generated by a source that is propagated through the liver. Liver stiffness increases systematically with stage of fibrosis; using a shear stiffness cut-off value of 2.93 kPa, the predicted sensitivity and specificity for detecting all grades of liver fibrosis is 98% and 99% respectively[84]. Malignant tumours have greater stiffness values than benign tumours and normal liver parenchyma[85-87]. Hence, MRE has shown to be a promising non-invasive tool for the imaging and characterization of solid hepatic tumours (Figure 15). A threshold value of approximately 5.0 kPa may be useful for differentiating benign focal lesions from malignant tumours[85]. The utility of MRE for differentiation of malignant tumors of liver is not well established and still under research.

MR spectroscopy

MR spectroscopy (MRS) allows for the non-invasive interrogation of the presence and concentration of various metabolites in tissue and hence aid in the provision of information with regards to tumour pathophysiology and metabolism[88]. It utilizes the magnetic properties of certain atomic nuclei; the more common ones employed are proton (^{1}H), phosphorus-31 (^{31}P) and carbon-13 (^{13}C). ^{1}H is the most commonly studied as it has the highest sensitivity. In liver tumour studies, the lactate resonance is related to energy metabolism of the tumour. Proton resonances of mobile lipids and the peak of total choline have been investigated as biomarkers to identify malignant tumours[88]. An increase in phosphomonoesters is associated with liver tumour progression and successful treatment is associated with a reduction of these levels[89-91]. Hence, ^{31}P MRS can potentially be used for treatment monitoring. MRS with ^{13}C has barely been utilized to examine human liver metabolism due to its technical complexity and relatively low sensitivity[88]. However, new techniques such as hyperpolarization

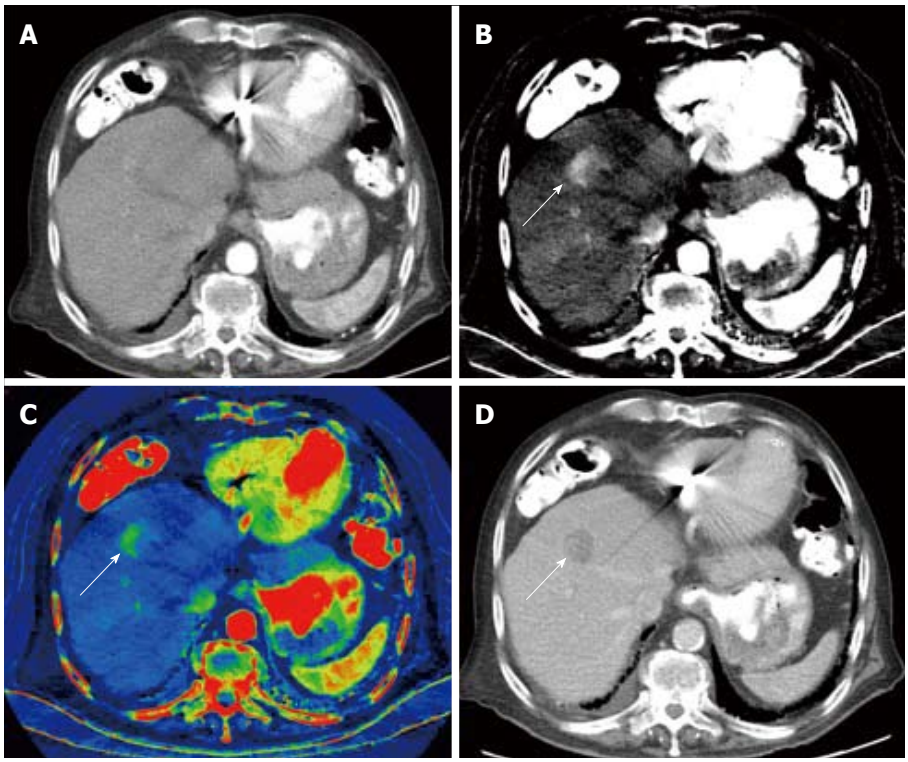

Figure 14 Dual-energy computed tomography of hepatocellular carcinoma. Nodular outline is suggestive of cirrhosis, arterial phase single energy computed tomography (SECT) image acquired at 140kVp demonstrates a vague focus of arterial enhancement that is difficult to differentiate from surrounding liver parenchyma (A), arterial phase DECT material decomposition iodine (MD-I) image shows uptake of iodine independently from inherent tissue attenuation, clearly demonstrating a nodular hyperenhancing lesion (B), arterial phase color overlay MD-I image also depicts the lesion well (C). Portal venous phase SECT image acquired at 120 kVp demonstrates characteristic wash-out (D). MD-I images improve detection and characterization of this small hepatocellular carcinoma. (Courtesy of Drs. Andrea Prochowski and Dushyant Sahani, Massachusetts General Hospital, Boston, MA, United States).

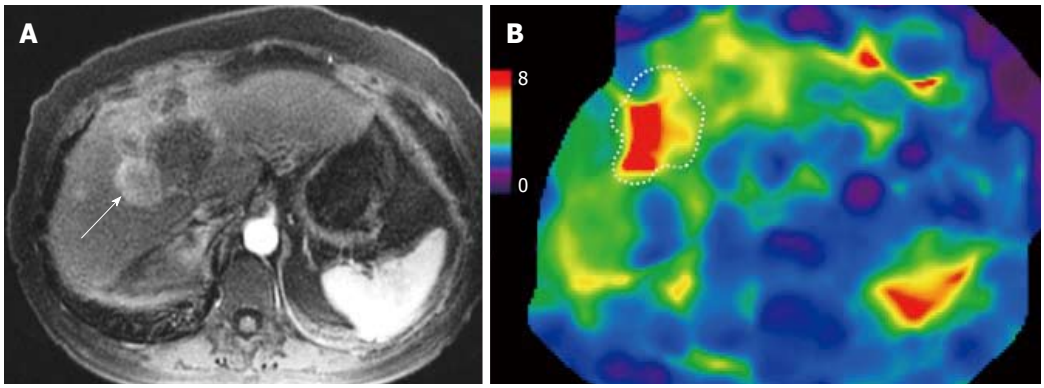

Figure 15 Magnetic resonance elastography of hepatocellular carcinoma. Arterial phase image (A) and stiffness map (B) from magnetic resonance elastography. The color scale of the stiffness map is expressed in kilopascal (kPa). A case of chronic alcoholic liver disease with liver stiffness of 5.3 kPa consistent with cirrhosis. The enhancing hepatocellular carcinoma (white arrow) has mean stiffness of 8.2 kPa suspicious for a malignant tumour. Note the tumor is stiffer in the more hyper enhancing regions of the tumour.

of ^{13}C-labeled glutamine has shown potential in the detection of small HCC in a cirrhotic liver[92].

Intravoxel incoherent motion imaging

DWI is a technique used for imaging molecular movement or diffusion. ADC in conventional DWI is influenced by two types of molecular movement: molecular diffusion and microcirculation in vessels (perfusion-related diffusion)[93]. With high *b*-values, the effect of perfusion-related diffusivity is largely eliminated and the ADC value can estimate true molecular diffusion. The effect of perfusion-related diffusion, however, cannot be completely removed. Hence, DWI performed using a range of low and high *b*-values or intravoxel incoherent motion imaging (IVIM) imaging has been employed to measure diffusion and perfusion-related diffusion separately[94,95]. Post processing of IVIM sequences can generate several

parameters including: the D value (true diffusion that reflects intra- and intercellular molecular movement) and the pseudo-diffusion coefficient D* which reflects the microcirculation in the vessels or perfusion-related diffusion; perfusion fraction (Pf) and ADC. D and D* aspects can be separated using biexponential fitting of the DWI data[95]. It is well-established that ADC values of malignant hepatic lesions are lower than that of benign lesions[96,97]. However, measured ADC values show substantial variability secondary to differences in choice of *b*-values[98]. Diffusivity values acquired using the IVIM model, however, are less influenced by the choice of *b*-values and may provide consistent and reproducible results[99]. Ichikawa *et al*[99] found that both the D and D* value of malignant hepatic lesions was suppressed compared with that of benign lesions and that the D value was a more reliable parameter between the two. IVIM-derived D values have been found to show significantly higher accuracy compared with ADC in differentiating high- from low-grade HCC[100]. Additionally, since D* reflects microcirculation, it may be possible to assess the effect of antiangiogenic drugs in HCC[101]. The early results show promise of IVIM in differentiating HCCs from benign nodules, however evidence for clinical utility is still lacking.

2-(^{18}F)fluoro-2-deoxy-D-galactose PET/CT

Positron emission tomography (PET) with the glucose analogue 2-(^{18}F)fluoro-2-deoxy-D-glucose (FDG) is extensively used in oncologic imaging. FDG-PET may be able to demonstrate increased uptake with HCC (Figure 10), however, it may miss 30%-50% of HCC lesions as the uptake is similar to the uptake in surrounding liver parenchyma[102-104]. Fluro-2-deoxy-D-Galagctose (FDGal) is touted as a hepatocyte-specific PET tracer for HCC; it is a tracer for galactose metabolism and avidly accumulates in the liver compared to other tissues[105]. It has potential not only as a PET tracer for detection of extra- but also intra-hepatic HCC. Sørensen *et al*[106] presented the first clinical study on the potential use of FDGal PET/CT for the detection of HCC and found high specificity in a retrospective study. Detection of HCC were comparable to that of multiphase contrast-enhanced CT. Additionally, FDGal PET/CT detected more nodules than other imaging modalities at the time of investigation and follow-up revealed rapid progression in those lesions. This may indicate the ability of FDGal to detect more lesions at earlier time points than conventional morphology based imaging modalities.

CONCLUSION

Imaging plays an imperative role in the diagnosis of HCC. The hallmark feature of arterial enhancement followed by washout is highly specific in at-risk patients and forms the foundation of current diagnostic guidelines. Difficulties in accurate diagnosis are largely secondary to lesions of small size. Ancillary features can aid in diagnosis and its use has been incorporated into Li-RADS. The use of hepatobiliary contrast agents has shown great promise in several studies with the ability to identify high grade dysplastic nodules and early HCC prior to neo-arterialization and progression to overt HCC, it may well be endorsed in future guidelines. Several other imaging techniques have also been investigated, many of which show potential that may shift the paradigm of HCC imaging assessment in the future.

REFERENCES

1 **Ferlay J**, Shin HR, Bray F, Forman D, Mathers C, Parkin DM. Estimates of worldwide burden of cancer in 2008: GLOBOCAN 2008. *Int J Cancer* 2010; **127**: 2893-2917 [PMID: 21351269 DOI: 10.1002/ijc.25516]

2 **Omata M**, Lesmana LA, Tateishi R, Chen PJ, Lin SM, Yoshida H, Kudo M, Lee JM, Choi BI, Poon RT, Shiina S, Cheng AL, Jia JD, Obi S, Han KH, Jafri W, Chow P, Lim SG, Chawla YK, Budihusodo U, Gani RA, Lesmana CR, Putranto TA, Liaw YF, Sarin SK. Asian Pacific Association for the Study of the Liver consensus recommendations on hepatocellular carcinoma. *Hepatol Int* 2010; **4**: 439-474 [PMID: 20827404 DOI: 10.1007/s12072-010-9165-7]

3 **El-Serag HB**, Rudolph KL. Hepatocellular carcinoma: epidemiology and molecular carcinogenesis. *Gastroenterology* 2007; **132**: 2557-2576 [PMID: 17570226 DOI: 10.1053/j.gastro.2007.04.061]

4 **van den Bos IC**, Hussain SM, Terkivatan T, Zondervan PE, de Man RA. Stepwise carcinogenesis of hepatocellular carcinoma in the cirrhotic liver: demonstration on serial MR imaging. *J Magn Reson Imaging* 2006; **24**: 1071-1080 [PMID: 17024654 DOI: 10.1002/jmri.20701]

5 **Simonetti RG**, Cammà C, Fiorello F, Politi F, D'Amico G, Pagliaro L. Hepatocellular carcinoma. A worldwide problem and the major risk factors. *Dig Dis Sci* 1991; **36**: 962-972 [PMID: 1649041 DOI: 10.1007/BF01297149]

6 **Ferenci P**, Fried M, Labrecque D, Bruix J, Sherman M, Omata M, Heathcote J, Piratsivuth T, Kew M, Otegbayo JA, Zheng SS, Sarin S, Hamid S, Modawi SB, Fleig W, Fedail S, Thomson A, Khan A, Malfertheiner P, Lau G, Carillo FJ, Krabshuis J, Le Mair A. World Gastroenterology Organisation Guideline. Hepatocellular carcinoma (HCC): a global perspective. *J Gastrointestin Liver Dis* 2010; **19**: 311-317 [PMID: 20922197 DOI: 10.1097/mcg.0b013e3181d46ef2]

7 **Polesel J**, Zucchetto A, Montella M, Dal Maso L, Crispo A, La Vecchia C, Serraino D, Franceschi S, Talamini R. The impact of obesity and diabetes mellitus on the risk of hepatocellular carcinoma. *Ann Oncol* 2009; **20**: 353-357 [PMID: 18723550 DOI: 10.1093/annonc/mdn565]

8 **Hung CH**, Chiu YC, Chen CH, Hu TH. MicroRNAs in hepatocellular carcinoma: carcinogenesis, progression, and therapeutic target. *Biomed Res Int* 2014; **2014**: 486407 [PMID: 24800233 DOI: 10.1155/2014/486407]

9 **Sanyal AJ**, Yoon SK, Lencioni R. The etiology of hepatocellular carcinoma and consequences for treatment. *Oncologist* 2010; **15** Suppl 4: 14-22 [PMID: 21115577 DOI: 10.1634/theoncologist.2010-S4-14]

10 **Montella M**, Crispo A, Giudice A. HCC, diet and metabolic factors: Diet and HCC. *Hepat Mon* 2011; **11**: 159-162 [PMID: 22087137]

11 **Trichopoulos D**, Bamia C, Lagiou P, Fedirko V, Trepo E, Jenab M, Pischon T, Nöthlings U, Overved K, Tjønneland A, Outzen M, Clavel-Chapelon F, Kaaks R, Lukanova A, Boeing H, Aleksandrova K, Benetou V, Zylis D, Palli D, Pala V, Panico S, Tumino R, Sacerdote C, Bueno-De-Mesquita HB, Van Kranen HJ, Peeters PH, Lund E, Quirós JR, González CA, Sanchez Perez MJ,

Navarro C, Dorronsoro M, Barricarte A, Lindkvist B, Regnér S, Werner M, Hallmans G, Khaw KT, Wareham N, Key T, Romieu I, Chuang SC, Murphy N, Boffetta P, Trichopoulou A, Riboli E. Hepatocellular carcinoma risk factors and disease burden in a European cohort: a nested case-control study. *J Natl Cancer Inst* 2011; **103**: 1686-1695 [PMID: 22021666 DOI: 10.1093/jnci/djr395]

12 **Marcellin P**, Pequignot F, Delarocque-Astagneau E, Zarski JP, Ganne N, Hillon P, Antona D, Bovet M, Mechain M, Asselah T, Desenclos JC, Jougla E. Mortality related to chronic hepatitis B and chronic hepatitis C in France: evidence for the role of HIV coinfection and alcohol consumption. *J Hepatol* 2008; **48**: 200-207 [PMID: 18086507]

13 **Dragani TA**. Risk of HCC: genetic heterogeneity and complex genetics. *J Hepatol* 2010; **52**: 252-257 [PMID: 20022654 10.1016/j.jhep.2009.11.015]

14 **Shiraha H**, Yamamoto K, Namba M. Human hepatocyte carcinogenesis (review). *Int J Oncol* 2013; **42**: 1133-1138 [PMID: 23426905 DOI: 10.3892/ijo.2013.1829]

15 **Hussain SM**, Semelka RC, Mitchell DG. MR imaging of hepatocellular carcinoma. *Magn Reson Imaging Clin N Am* 2002; **10**: 31-52, v [PMID: 11998574 DOI: 10.1016/S1064-9689(03)00048-5]

16 **Ronot M**, Vilgrain V. Hepatocellular carcinoma: diagnostic criteria by imaging techniques. *Best Pract Res Clin Gastroenterol* 2014; **28**: 795-812 [PMID: 25260309 DOI: 10.1016/j.bpg.2014.08.005]

17 **Choi JY**, Lee JM, Sirlin CB. CT and MR imaging diagnosis and staging of hepatocellular carcinoma: part I. Development, growth, and spread: key pathologic and imaging aspects. *Radiology* 2014; **272**: 635-654 [PMID: 25153274 DOI: 10.1148/radiol.14132361]

18 **International Working Party**. Terminology of nodular hepatocellular lesions. *Hepatology* 1995; **22**: 983-993 [PMID: 7657307 DOI: 10.1002/hep.1840220341]

19 **Park YN**, Kim MJ. Hepatocarcinogenesis: imaging-pathologic correlation. *Abdom Imaging* 2011; **36**: 232-243 [PMID: 21267560 DOI: 10.1007/s00261-011-9688-y]

20 **Krinsky GA**, Lee VS, Nguyen MT, Rofsky NM, Theise ND, Morgan GR, Teperman LW, Weinreb JC. Siderotic nodules at MR imaging: regenerative or dysplastic? *J Comput Assist Tomogr* 2000; **24**: 773-776 [PMID: 11045701]

21 **Xu PJ**, Yan FH, Wang JH, Shan Y, Ji Y, Chen CZ. Contribution of diffusion-weighted magnetic resonance imaging in the characterization of hepatocellular carcinomas and dysplastic nodules in cirrhotic liver. *J Comput Assist Tomogr* 2010; **34**: 506-512 [PMID: 20657216 DOI: 10.1097/RCT.0b013e3181da3671]

22 **Krinsky GA**, Israel G. Nondysplastic nodules that are hyperintense on T1-weighted gradient-echo MR imaging: frequency in cirrhotic patients undergoing transplantation. *AJR Am J Roentgenol* 2003; **180**: 1023-1027 [PMID: 12646448 DOI: 10.1097/00004728-200009000-00019]

23 **Hanna RF**, Aguirre DA, Kased N, Emery SC, Peterson MR, Sirlin CB. Cirrhosis-associated hepatocellular nodules: correlation of histopathologic and MR imaging features. *Radiographics* 2008; **28**: 747-769 [PMID: 18480482 DOI: 10.1148/rg.283055108]

24 **Park YN**. Update on precursor and early lesions of hepatocellular carcinomas. *Arch Pathol Lab Med* 2011; **135**: 704-715 [PMID: 21631263 DOI: 10.1043/2010-0524-RA.1]

25 **International Consensus Group for Hepatocellular Neoplasia**. Pathologic diagnosis of early hepatocellular carcinoma: a report of the international consensus group for hepatocellular neoplasia. *Hepatology* 2009; **49**: 658-664 [PMID: 19177576 DOI: 10.1002/hep.22709]

26 **Bruix J**, Sherman M. Management of hepatocellular carcinoma. *Hepatology* 2005; **42**: 1208-1236 [PMID: 16250051 DOI: 10.1002/hep.20933]

27 **Roskams T**, Kojiro M. Pathology of early hepatocellular carcinoma: conventional and molecular diagnosis. *Semin Liver Dis* 2010; **30**: 17-25 [PMID: 20175030 DOI: 10.1055/s-0030-1247129]

28 **Lim JH**, Choi BI. Dysplastic nodules in liver cirrhosis: imaging. *Abdom Imaging* 2002; **27**: 117-128 [PMID: 11847571 DOI: 10.1007/s00261-001-0088-6]

29 **Martín J**, Sentís M, Zidan A, Donoso L, Puig J, Falcó J, Bella R. Fatty metamorphosis of hepatocellular carcinoma: detection with chemical shift gradient-echo MR imaging. *Radiology* 1995; **195**: 125-130 [PMID: 7892452 DOI: 10.1148/radiology.195.1.7892452]

30 **Willatt JM**, Hussain HK, Adusumilli S, Marrero JA. MR Imaging of hepatocellular carcinoma in the cirrhotic liver: challenges and controversies. *Radiology* 2008; **247**: 311-330 [PMID: 18430871 DOI: 10.1148/radiol.2472061331]

31 **Park MJ**, Kim YK, Lee MH, Lee JH. Validation of diagnostic criteria using gadoxetic acid-enhanced and diffusion-weighted MR imaging for small hepatocellular carcinoma (& lt; = 2.0 cm) in patients with hepatitis-induced liver cirrhosis. *Acta Radiol* 2013; **54**: 127-136 [PMID: 23148300 DOI: 10.1258/ar.2012.120262]

32 **Sakamoto M**. Pathology of early hepatocellular carcinoma. *Hepatol Res* 2007; **37** Suppl 2: S135-S138 [PMID: 17877474 DOI: 10.1111/j.1872-034X.2007.00176.x]

33 **Stevens WR**, Gulino SP, Batts KP, Stephens DH, Johnson CD. Mosaic pattern of hepatocellular carcinoma: histologic basis for a characteristic CT appearance. *J Comput Assist Tomogr* 1996; **20**: 337-342 [PMID: 8626886 DOI: 10.1097/00004728-199605000-00001]

34 **European Association for the Study of the Liver, European Organization for Research and Treatment of Cancer**. EASL-EORTC clinical practice guidelines: management of hepatocellular carcinoma. *J Hepatol* 2012; **56**: 908-943 [PMID: 22424438 DOI: 10.1016/j.jhep.2011.12.001]

35 **Bruix J**, Sherman M. Management of hepatocellular carcinoma: an update. *Hepatology* 2011; **53**: 1020-1022 [PMID: 21374666 DOI: 10.1002/hep.24199]

36 **Forner A**, Vilana R, Ayuso C, Bianchi L, Solé M, Ayuso JR, Boix L, Sala M, Varela M, Llovet JM, Brú C, Bruix J. Diagnosis of hepatic nodules 20 mm or smaller in cirrhosis: Prospective validation of the noninvasive diagnostic criteria for hepatocellular carcinoma. *Hepatology* 2008; **47**: 97-104 [PMID: 18069697 DOI: 10.1002/hep.21966]

37 **Carlos RC**, Kim HM, Hussain HK, Francis IR, Nghiem HV, Fendrick AM. Developing a prediction rule to assess hepatic malignancy in patients with cirrhosis. *AJR Am J Roentgenol* 2003; **180**: 893-900 [PMID: 12646426 DOI: 10.2214/ajr.180.4.1800893]

38 **Marrero JA**, Hussain HK, Nghiem HV, Umar R, Fontana RJ, Lok AS. Improving the prediction of hepatocellular carcinoma in cirrhotic patients with an arterially-enhancing liver mass. *Liver Transpl* 2005; **11**: 281-289 [PMID: 15719410 DOI: 10.1002/lt.20357]

39 **Semelka RC**, Martin DR, Balci C, Lance T. Focal liver lesions: comparison of dual-phase CT and multisequence multiplanar MR imaging including dynamic gadolinium enhancement. *J Magn Reson Imaging* 2001; **13**: 397-401 [PMID: 11241813 DOI: 10.1002/jmri.1057]

40 **Kim YK**, Kim CS, Chung GH, Han YM, Lee SY, Chon SB, Lee JM. Comparison of gadobenate dimeglumine-enhanced dynamic MRI and 16-MDCT for the detection of hepatocellular carcinoma. *AJR Am J Roentgenol* 2006; **186**: 149-157 [PMID: 16357395 DOI: 10.2214/AJR.04.1206]

41 **Sersté T**, Barrau V, Ozenne V, Vullierme MP, Bedossa P, Farges O, Valla DC, Vilgrain V, Paradis V, Degos F. Accuracy and disagreement of computed tomography and magnetic resonance imaging for the diagnosis of small hepatocellular carcinoma and dysplastic nodules: role of biopsy. *Hepatology* 2012; **55**: 800-806 [PMID: 22006503 DOI: 10.1002/hep.24746]

42 **Rimola J**, Forner A, Tremosini S, Reig M, Vilana R, Bianchi L, Rodríguez-Lope C, Solé M, Ayuso C, Bruix J. Non-invasive diagnosis of hepatocellular carcinoma ≤ 2 cm in cirrhosis. Diagnostic accuracy assessing fat, capsule and signal intensity at dynamic MRI. *J Hepatol* 2012; **56**: 1317-1323 [PMID: 22314420 DOI: 10.1016/j.jhep.2012.01.004]

43 **Rode A**, Bancel B, Douek P, Chevallier M, Vilgrain V, Picaud G, Henry L, Berger F, Bizollon T, Gaudin JL, Ducerf C. Small nodule detection in cirrhotic livers: evaluation with US, spiral

CT, and MRI and correlation with pathologic examination of explanted liver. *J Comput Assist Tomogr* 2001; **25**: 327-336 [PMID: 11351179 DOI: 10.1097/00004728-200105000-00001]
44 **Liu K**, He X, Lei XZ, Zhao LS, Tang H, Liu L, Lei BJ. Pathomorphological study on location and distribution of Kupffer cells in hepatocellular carcinoma. *World J Gastroenterol* 2003; **9**: 1946-1949 [PMID: 12970881 DOI: 10.3748/wjg.v9.i9.1946]
45 **Radiology ACo**. Liver imaging reporting and data system version v 2013.1. (Accessed May 12, 2014). Available from: URL: http://www.acr.org/Quality-Safety/Resources/LIRADS/
46 **Kim MJ**. Current limitations and potential breakthroughs for the early diagnosis of hepatocellular carcinoma. *Gut Liver* 2011; **5**: 15-21 [PMID: 21461067 DOI: 10.5009/gnl.2011.5.1.15]
47 **Rosenkrantz AB**, Lee L, Matza BW, Kim S. Infiltrative hepatocellular carcinoma: comparison of MRI sequences for lesion conspicuity. *Clin Radiol* 2012; **67**: e105-e111 [PMID: 23026725 DOI: 10.1016/j.crad.2012.08.019]
48 **Yu JS**, Lee JH, Chung JJ, Kim JH, Kim KW. Small hypervascular hepatocellular carcinoma: limited value of portal and delayed phases on dynamic magnetic resonance imaging. *Acta Radiol* 2008; **49**: 735-743 [PMID: 18608015 DOI: 10.1080/02841850802120045]
49 **Khan AS**, Hussain HK, Johnson TD, Weadock WJ, Pelletier SJ, Marrero JA. Value of delayed hypointensity and delayed enhancing rim in magnetic resonance imaging diagnosis of small hepatocellular carcinoma in the cirrhotic liver. *J Magn Reson Imaging* 2010; **32**: 360-366 [PMID: 20677263 DOI: 10.1002/jmri.22271]
50 **Sandrasegaran K**, Tahir B, Patel A, Ramaswamy R, Bertrand K, Akisik FM, Saxena R. The usefulness of diffusion-weighted imaging in the characterization of liver lesions in patients with cirrhosis. *Clin Radiol* 2013; **68**: 708-715 [PMID: 23510619 DOI: 10.1016/j.crad.2012.10.023]
51 **Piana G**, Trinquart L, Meskine N, Barrau V, Beers BV, Vilgrain V. New MR imaging criteria with a diffusion-weighted sequence for the diagnosis of hepatocellular carcinoma in chronic liver diseases. *J Hepatol* 2011; **55**: 126-132 [PMID: 21145857 DOI: 10.1016/j.jhep.2010.10.023]
52 **Vandecaveye V**, De Keyzer F, Verslype C, Op de Beeck K, Komuta M, Topal B, Roebben I, Bielen D, Roskams T, Nevens F, Dymarkowski S. Diffusion-weighted MRI provides additional value to conventional dynamic contrast-enhanced MRI for detection of hepatocellular carcinoma. *Eur Radiol* 2009; **19**: 2456-2466 [PMID: 19440718 DOI: 10.1007/s00330-009-1431-5]
53 **Wu LM**, Xu JR, Lu Q, Hua J, Chen J, Hu J. A pooled analysis of diffusion-weighted imaging in the diagnosis of hepatocellular carcinoma in chronic liver diseases. *J Gastroenterol Hepatol* 2013; **28**: 227-234 [PMID: 23190006 DOI: 10.1111/jgh.12054]
54 **Taouli B**, Koh DM. Diffusion-weighted MR imaging of the liver. *Radiology* 2010; **254**: 47-66 [PMID: 20032142 DOI: 10.1148/radiol.09090021]
55 **Siripongsakun S**, Lee JK, Raman SS, Tong MJ, Sayre J, Lu DS. MRI detection of intratumoral fat in hepatocellular carcinoma: potential biomarker for a more favorable prognosis. *AJR Am J Roentgenol* 2012; **199**: 1018-1025 [PMID: 23096174 DOI: 10.2214/AJR.12.8632]
56 **Ebara M**, Fukuda H, Kojima Y, Morimoto N, Yoshikawa M, Sugiura N, Satoh T, Kondo F, Yukawa M, Matsumoto T, Saisho H. Small hepatocellular carcinoma: relationship of signal intensity to histopathologic findings and metal content of the tumor and surrounding hepatic parenchyma. *Radiology* 1999; **210**: 81-88 [PMID: 9885591 DOI: 10.1148/radiology.210.1.r99ja4181]
57 **Okuda K**, Musha H, Nakajima Y, Kubo Y, Shimokawa Y, Nagasaki Y, Sawa Y, Jinnouchi S, Kaneko T, Obata H, Hisamitsu T, Motoike Y, Okazaki N, Kojiro M, Sakamoto K, Nakashima T. Clinicopathologic features of encapsulated hepatocellular carcinoma: a study of 26 cases. *Cancer* 1977; **40**: 1240-1245 [PMID: 198091 DOI: 10.1002/1097-0142(197709)40:3]
58 **Ng IO**, Lai EC, Ng MM, Fan ST. Tumor encapsulation in hepatocellular carcinoma. A pathologic study of 189 cases. *Cancer* 1992; **70**: 45-49 [PMID: 1318778]
59 **Ros PR**, Murphy BJ, Buck JL, Olmedilla G, Goodman Z. Encapsulated hepatocellular carcinoma: radiologic findings and pathologic correlation. *Gastrointest Radiol* 1990; **15**: 233-237 [PMID: 2160391 DOI: 10.1007/BF01888783]
60 **Okuda K**. Hepatocellular carcinoma: clinicopathological aspects. *J Gastroenterol Hepatol* 1997; **12**: S314-S318 [PMID: 9407352 DOI: 10.1111/j.1440-1746.1997.tb00515.x]
61 **Shah ZK**, McKernan MG, Hahn PF, Sahani DV. Enhancing and expansile portal vein thrombosis: value in the diagnosis of hepatocellular carcinoma in patients with multiple hepatic lesions. *AJR Am J Roentgenol* 2007; **188**: 1320-1323 [PMID: 17449777]
62 **Kitao A**, Matsui O, Yoneda N, Kozaka K, Shinmura R, Koda W, Kobayashi S, Gabata T, Zen Y, Yamashita T, Kaneko S, Nakanuma Y. The uptake transporter OATP8 expression decreases during multistep hepatocarcinogenesis: correlation with gadoxetic acid enhanced MR imaging. *Eur Radiol* 2011; **21**: 2056-2066 [PMID: 21626360 DOI: 10.1007/s00330-011-2165-8]
63 **Tanimoto A**, Higuchi N, Ueno A. Reduction of ringing artifacts in the arterial phase of gadoxetic acid-enhanced dynamic MR imaging. *Magn Reson Med Sci* 2012; **11**: 91-97 [PMID: 22790295 DOI: 10.2463/mrms.11.91]
64 **Tanimoto A**, Lee JM, Murakami T, Huppertz A, Kudo M, Grazioli L. Consensus report of the 2nd International Forum for Liver MRI. *Eur Radiol* 2009; **19** Suppl 5: S975-S989 [PMID: 19851766 DOI: 10.1007/s00330-009-1624-y]
65 **Nakamura Y**, Toyota N, Date S, Oda S, Namimoto T, Yamashita Y, Beppu T, Awai K. Clinical significance of the transitional phase at gadoxetate disodium-enhanced hepatic MRI for the diagnosis of hepatocellular carcinoma: preliminary results. *J Comput Assist Tomogr* 2011; **35**: 723-727 [PMID: 22082543 DOI: 10.1097/RCT.0b013e3182372c40]
66 **Sano K**, Ichikawa T, Motosugi U, Sou H, Muhi AM, Matsuda M, Nakano M, Sakamoto M, Nakazawa T, Asakawa M, Fujii H, Kitamura T, Enomoto N, Araki T. Imaging study of early hepatocellular carcinoma: usefulness of gadoxetic acid-enhanced MR imaging. *Radiology* 2011; **261**: 834-844 [PMID: 21998047 DOI: 10.1148/radiol.11101840]
67 **Lee SA**, Lee CH, Jung WY, Lee J, Choi JW, Kim KA, Park CM. Paradoxical high signal intensity of hepatocellular carcinoma in the hepatobiliary phase of Gd-EOB-DTPA enhanced MRI: initial experience. *Magn Reson Imaging* 2011; **29**: 83-90 [PMID: 20832227 DOI: 10.1016/j.mri.2010.07.019]
68 **Tsuboyama T**, Onishi H, Kim T, Akita H, Hori M, Tatsumi M, Nakamoto A, Nagano H, Matsuura N, Wakasa K, Tomoda K. Hepatocellular carcinoma: hepatocyte-selective enhancement at gadoxetic acid-enhanced MR imaging--correlation with expression of sinusoidal and canalicular transporters and bile accumulation. *Radiology* 2010; **255**: 824-833 [PMID: 20501720 DOI: 10.1148/radiol.10091557]
69 **Ahn SS**, Kim MJ, Lim JS, Hong HS, Chung YE, Choi JY. Added value of gadoxetic acid-enhanced hepatobiliary phase MR imaging in the diagnosis of hepatocellular carcinoma. *Radiology* 2010; **255**: 459-466 [PMID: 20413759 DOI: 10.1148/radiol.10091388]
70 **Golfieri R**, Renzulli M, Lucidi V, Corcioni B, Trevisani F, Bolondi L. Contribution of the hepatobiliary phase of Gd-EOB-DTPA-enhanced MRI to Dynamic MRI in the detection of hypovascular small (≤ 2 cm) HCC in cirrhosis. *Eur Radiol* 2011; **21**: 1233-1242 [PMID: 21293864 DOI: 10.1007/s00330-010-2030-1]
71 **Marin D**, Di Martino M, Guerrisi A, De Filippis G, Rossi M, Ginanni Corradini S, Masciangelo R, Catalano C, Passariello R. Hepatocellular carcinoma in patients with cirrhosis: qualitative comparison of gadobenate dimeglumine-enhanced MR imaging and multiphasic 64-section CT. *Radiology* 2009; **251**: 85-95 [PMID: 19332848 DOI: 10.1148/radiol.2511080400]
72 **Choi JW**, Lee JM, Kim SJ, Yoon JH, Baek JH, Han JK, Choi BI. Hepatocellular carcinoma: imaging patterns on gadoxetic acid-enhanced MR Images and their value as an imaging biomarker. *Radiology* 2013; **267**: 776-786 [PMID: 23401584 DOI: 10.1148/radiol.13120775]
73 **Hennedige T**, Yang ZJ, Ong CK, Venkatesh SK. Utility of

non-contrast-enhanced CT for improved detection of arterial phase hyperenhancement in hepatocellular carcinoma. *Abdom Imaging* 2014; **39**: 1247-1254 [PMID: 24943135 DOI: 10.1007/s00261-014-0174-1]
74 **Singh J**, Sharma S, Aggarwal N, Sood RG, Sood S, Sidhu R. Role of Perfusion CT Differentiating Hemangiomas from Malignant Hepatic Lesions. *J Clin Imaging Sci* 2014; **4**: 10 [PMID: 24744967 DOI: 10.4103/2156-7514.127959]
75 **Sahani DV**, Holalkere NS, Mueller PR, Zhu AX. Advanced hepatocellular carcinoma: CT perfusion of liver and tumor tissue--initial experience. *Radiology* 2007; **243**: 736-743 [PMID: 17517931 DOI: 10.1148/radiol.2433052020]
76 **Ippolito D**, Sironi S, Pozzi M, Antolini L, Invernizzi F, Ratti L, Leone EB, Fazio F. Perfusion CT in cirrhotic patients with early stage hepatocellular carcinoma: assessment of tumor-related vascularization. *Eur J Radiol* 2010; **73**: 148-152 [PMID: 19054640 DOI: 10.1016/j.ejrad.2008.10.014]
77 **Bayraktutan Ü**, Kantarci A, Oğul H, Kizrak Y, Özyiğit Ö, Yüceler Z, Genç B, Özoğul B. Evaluation of hepatocellular carcinoma with computed tomography perfusion imaging. *Turk J Med Sci* 2014; **44**: 193-196 [PMID: 25536723 DOI: 10.3906/sag-1303-27]
78 **Goh V**, Ng QS, Miles K. Computed tomography perfusion imaging for therapeutic assessment: has it come of age as a biomarker in oncology? *Invest Radiol* 2012; **47**: 2-4 [PMID: 21808202 DOI: 10.1097/RLI.0b013e318229ff3e]
79 **Postma AA**, Das M, Stadler AA, Wildberger JE. Dual-Energy CT: What the Neuroradiologist Should Know. *Curr Radiol Rep* 2015; **3**: 16 [PMID: 25815242 DOI: 10.1007/s40134-015-0097-9]
80 **Okada M**, Kim T, Murakami T. Hepatocellular nodules in liver cirrhosis: state of the art CT evaluation (perfusion CT/volume helical shuttle scan/dual-energy CT, etc.). *Abdom Imaging* 2011; **36**: 273-281 [PMID: 21267563 DOI: 10.1007/s00261-011-9684-2]
81 **Gao SY**, Zhang XP, Cui Y, Sun YS, Tang L, Li XT, Zhang XY, Shan J. Fused monochromatic imaging acquired by single source dual energy CT in hepatocellular carcinoma during arterial phase: an initial experience. *Chin J Cancer Res* 2014; **26**: 437-443 [PMID: 25232217 DOI: 10.3978/j.issn.1000-9604.2014.08.15]
82 **Davarpanah AH**, Weinreb JC. The role of imaging in hepatocellular carcinoma: the present and future. *J Clin Gastroenterol* 2013; **47** Suppl: S7-10 [PMID: 23632342 DOI: 10.1097/MCG.0b013e31827f0d3d]
83 **Huwart L**, Peeters F, Sinkus R, Annet L, Salameh N, ter Beek LC, Horsmans Y, Van Beers BE. Liver fibrosis: non-invasive assessment with MR elastography. *NMR Biomed* 2006; **19**: 173-179 [PMID: 16521091 DOI: 10.1002/nbm.1030]
84 **Yin M**, Talwalkar JA, Glaser KJ, Manduca A, Grimm RC, Rossman PJ, Fidler JL, Ehman RL. Assessment of hepatic fibrosis with magnetic resonance elastography. *Clin Gastroenterol Hepatol* 2007; **5**: 1207-1213.e2 [PMID: 17916548 DOI: 10.1016/j.cgh.2007.06.012]
85 **Venkatesh SK**, Yin M, Glockner JF, Takahashi N, Araoz PA, Talwalkar JA, Ehman RL. MR elastography of liver tumors: preliminary results. *AJR Am J Roentgenol* 2008; **190**: 1534-1540 [PMID: 18492904 DOI: 10.2214/AJR.07.3123]
86 **Garteiser P**, Doblas S, Daire JL, Wagner M, Leitao H, Vilgrain V, Sinkus R, Van Beers BE. MR elastography of liver tumours: value of viscoelastic properties for tumour characterisation. *Eur Radiol* 2012; **22**: 2169-2177 [PMID: 22572989 DOI: 10.1007/s00330-012-2474-6]
87 **Hennedige TP**, Hallinan TP, Leung FP, Teo LLS, Iyer S, Wang G, Chang S, Madhavan K, Wee A, Venkatesh SK. Comparison of magnetic resonance elastography and diffusion-weighted imaging for differentiating benign and malignant liver lesions. *Eur Radiol* 2015; Epub ahead of print [PMID: 26032879 DOI: 10.1007/s00330-015-3835-8]
88 **ter Voert EG**, Heijmen L, van Laarhoven HW, Heerschap A. In vivo magnetic resonance spectroscopy of liver tumors and metastases. *World J Gastroenterol* 2011; **17**: 5133-5149 [PMID: 22215937 DOI: 10.3748/wjg.v17.i47.5133]
89 **Bell JD**, Cox IJ, Sargentoni J, Peden CJ, Menon DK, Foster CS, Watanapa P, Iles RA, Urenjak J. A 31P and 1H-NMR investigation in vitro of normal and abnormal human liver. *Biochim Biophys Acta* 1993; **1225**: 71-77 [PMID: 8241291 DOI: 10.1016/0925-4439(93)90124-J]
90 **Meyerhoff DJ**, Karczmar GS, Valone F, Venook A, Matson GB, Weiner MW. Hepatic cancers and their response to chemoembolization therapy. Quantitative image-guided 31P magnetic resonance spectroscopy. *Invest Radiol* 1992; **27**: 456-464 [PMID: 1318873 DOI: 10.1097/00004424-199206000-00011]
91 **Negendank W**. Studies of human tumors by MRS: a review. *NMR Biomed* 1992; **5**: 303-324 [PMID: 1333263 DOI: 10.1002/nbm.1940050518]
92 **Gallagher FA**, Kettunen MI, Day SE, Lerche M, Brindle KM. 13C MR spectroscopy measurements of glutaminase activity in human hepatocellular carcinoma cells using hyperpolarized 13C-labeled glutamine. *Magn Reson Med* 2008; **60**: 253-257 [PMID: 18666104 DOI: 10.1002/mrm.21650]
93 **Le Bihan D**, Breton E, Lallemand D, Grenier P, Cabanis E, Laval-Jeantet M. MR imaging of intravoxel incoherent motions: application to diffusion and perfusion in neurologic disorders. *Radiology* 1986; **161**: 401-407 [PMID: 3763909 DOI: 10.1148/radiology.161.2.3763909]
94 **Thoeny HC**, Zumstein D, Simon-Zoula S, Eisenberger U, De Keyzer F, Hofmann L, Vock P, Boesch C, Frey FJ, Vermathen P. Functional evaluation of transplanted kidneys with diffusion-weighted and BOLD MR imaging: initial experience. *Radiology* 2006; **241**: 812-821 [PMID: 17114628 DOI: 10.1148/radiol.2413060103]
95 **Thoeny HC**, De Keyzer F. Diffusion-weighted MR imaging of native and transplanted kidneys. *Radiology* 2011; **259**: 25-38 [PMID: 21436095 DOI: 10.1148/radiol.10092419]
96 **Nasu K**, Kuroki Y, Tsukamoto T, Nakajima H, Mori K, Minami M. Diffusion-weighted imaging of surgically resected hepatocellular carcinoma: imaging characteristics and relationship among signal intensity, apparent diffusion coefficient, and histopathologic grade. *AJR Am J Roentgenol* 2009; **193**: 438-444 [PMID: 19620441 DOI: 10.2214/AJR.08.1424]
97 **Yamada I**, Aung W, Himeno Y, Nakagawa T, Shibuya H. Diffusion coefficients in abdominal organs and hepatic lesions: evaluation with intravoxel incoherent motion echo-planar MR imaging. *Radiology* 1999; **210**: 617-623 [PMID: 10207458 DOI: 10.1148/radiology.210.3.r99fe17617]
98 **Taouli B**, Vilgrain V, Dumont E, Daire JL, Fan B, Menu Y. Evaluation of liver diffusion isotropy and characterization of focal hepatic lesions with two single-shot echo-planar MR imaging sequences: prospective study in 66 patients. *Radiology* 2003; **226**: 71-78 [PMID: 12511671 DOI: 10.1148/radiol.2261011904]
99 **Ichikawa S**, Motosugi U, Ichikawa T, Sano K, Morisaka H, Araki T. Intravoxel incoherent motion imaging of focal hepatic lesions. *J Magn Reson Imaging* 2013; **37**: 1371-1376 [PMID: 23172819 DOI: 10.1002/jmri.23930]
100 **Woo S**, Lee JM, Yoon JH, Joo I, Han JK, Choi BI. Intravoxel incoherent motion diffusion-weighted MR imaging of hepatocellular carcinoma: correlation with enhancement degree and histologic grade. *Radiology* 2014; **270**: 758-767 [PMID: 24475811 DOI: 10.1148/radiol.13130444]
101 **Lewin M**, Fartoux L, Vignaud A, Arrivé L, Menu Y, Rosmorduc O. The diffusion-weighted imaging perfusion fraction f is a potential marker of sorafenib treatment in advanced hepatocellular carcinoma: a pilot study. *Eur Radiol* 2011; **21**: 281-290 [PMID: 20683597 DOI: 10.1007/s00330-010-1914-4]
102 **Khan MA**, Combs CS, Brunt EM, Lowe VJ, Wolverson MK, Solomon H, Collins BT, Di Bisceglie AM. Positron emission tomography scanning in the evaluation of hepatocellular carcinoma. *J Hepatol* 2000; **32**: 792-797 [PMID: 10845666 DOI: 10.1016/S0168-8278(00)80248-2]
103 **Delbeke D**, Martin WH. Update of PET and PET/CT for hepatobiliary and pancreatic malignancies. *HPB* (Oxford) 2005; **7**: 166-179 [PMID: 18333185 DOI: 10.1080/13651820510028909]
104 **Wudel LJ**, Delbeke D, Morris D, Rice M, Washington MK, Shyr Y, Pinson CW, Chapman WC. The role of [18F]fluorodeoxyglucose

positron emission tomography imaging in the evaluation of hepatocellular carcinoma. *Am Surg* 2003; **69**: 117-124; discussion 124-126 [PMID: 12641351]

105 **Sørensen M**, Munk OL, Mortensen FV, Olsen AK, Bender D, Bass L, Keiding S. Hepatic uptake and metabolism of galactose can be quantified in vivo by 2-[18F]fluoro-2-deoxygalactose positron emission tomography. *Am J Physiol Gastrointest Liver Physiol* 2008; **295**: G27-G36 [PMID: 18483186 DOI: 10.1152/ajpgi.00004.2008]

106 **Sørensen M**, Frisch K, Bender D, Keiding S. The potential use of 2-[^{18}F]fluoro-2-deoxy-D-galactose as a PET/CT tracer for detection of hepatocellular carcinoma. *Eur J Nucl Med Mol Imaging* 2011; **38**: 1723-1731 [PMID: 21553087 DOI: 10.1007/s00259-011-1831-z]

P- Reviewer: Lam V, Sicklick JK, Yang T **S- Editor**: Yu J
L- Editor: A **E- Editor**: Wang CH

Published by **Baishideng Publishing Group Inc**
8226 Regency Drive, Pleasanton, CA 94588, USA
Telephone: +1-925-223-8242
Fax: +1-925-223-8243
E-mail: bpgoffice@wjgnet.com
Help Desk: http://www.wjgnet.com/esps/helpdesk.aspx
http://www.wjgnet.com

ISSN 1007-9327